



HAL
open science

Ecological Modeling for the Extrapolation of Ecotoxicological Effects Measured during in Situ Assays in Gammarus

Romain Coulaud, Olivier Geffard, A Coquillat, H. Quéau, Sandrine Charles,
Arnaud Chaumot

► **To cite this version:**

Romain Coulaud, Olivier Geffard, A Coquillat, H. Quéau, Sandrine Charles, et al.. Ecological Modeling for the Extrapolation of Ecotoxicological Effects Measured during in Situ Assays in Gammarus. Environmental Science and Technology, 2014, 48 (11), pp.6428-6436. 10.1021/es501126g. hal-01191544

HAL Id: hal-01191544

<https://hal.science/hal-01191544v1>

Submitted on 2 Sep 2015

HAL is a multi-disciplinary open access archive for the deposit and dissemination of scientific research documents, whether they are published or not. The documents may come from teaching and research institutions in France or abroad, or from public or private research centers.

L'archive ouverte pluridisciplinaire **HAL**, est destinée au dépôt et à la diffusion de documents scientifiques de niveau recherche, publiés ou non, émanant des établissements d'enseignement et de recherche français ou étrangers, des laboratoires publics ou privés.

1 Ecological modelling for the extrapolation of
2 ecotoxicological effects measured during *in situ*
3 assays in *Gammarus*.

4

5 *Romain Coulaud*^{§, #}, *Olivier Geffard*[§], *Amandine Coquillat*[§], *Hervé Quéau*[§], *Sandrine*
6 *Charles*^{#, □}, *Arnaud Chaumot*^{*, §}

7

8 § Irstea, UR MALY, F-69626 Villeurbanne, France.

9 # Université de Lyon, F-69000, Lyon ; Université Lyon 1 ; CNRS, UMR5558, Laboratoire de
10 Biométrie et Biologie Evolutive, F-69622 Villeurbanne, France.

11 □ Institut Universitaire de France, 103, bd Saint-Michel, 75005 Paris, France

12

13 **KEYWORDS**

14 *Gammarus fossarum*, life-history, biomonitoring, population models, effect upscaling

15

16 **ABSTRACT**

17 Evaluating the effects of chemical contamination on populations and ecological
18 communities still constitutes a challenging necessity in environmental management. However
19 the toxic effects of contaminants are commonly measured by means of organism-level
20 responses. Linking such effects measures with ecological models is a promising way to
21 apprehend population-level impacts. In this way, population models are currently increasingly
22 used in predictive risk assessment procedures, but their use in environmental diagnostic
23 framework remains limited due to their lack of ecological realism. The present study with the
24 crustacean *Gammarus fossarum*, a sentinel species in freshwater monitoring, combines a dual
25 field and laboratory experimental approach with a population modelling framework. In this
26 way, we developed an ecologically-relevant periodic matrix population model for *Gammarus*.
27 This model allowed us to capture the population dynamics in the field, and to understand the
28 particular pattern of demographic sensitivities induced by *Gammarus* life-history phenology.
29 The model we developed provided a robust population-level assessment of *in situ*-based
30 effects measures recorded during a biomonitoring program on a French watershed impacted
31 by past mining activities. Thus, our study illustrates the potential of population modelling
32 when seeking to decipher the role of environmental toxic contamination in ecological
33 perturbations.

34

35

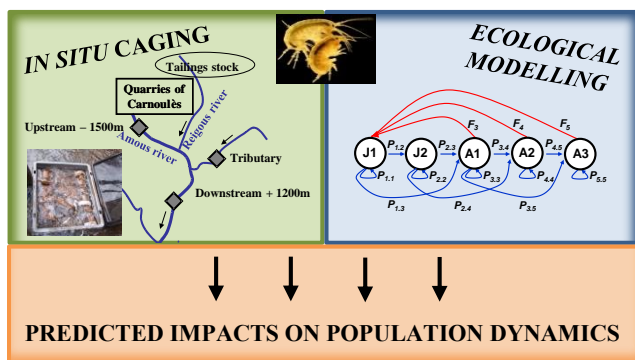
36

37

38

39

40 **TOC/Abstract graphic**



41

42

43 1. INTRODUCTION

44 In order to understand the role of chemical contamination in the degradation of
45 environmental quality, the ecotoxicological approach studies the sub-lethal effects of
46 contaminants by means of sub-individual biomarkers or individual responses. One can thus
47 focus the diagnostic assessment at lower levels of biological organization compared to
48 integrated ecological impact studies on populations, communities and ecosystem functioning
49 ¹⁻⁴. These organism-level markers are expected to be specific and sensitive to the toxic effects
50 of contaminants. They are therefore used to gain insights into causal relationships between
51 contamination and biological impacts, an essential step in proposing relevant environmental
52 management programs. Nevertheless, their ecological relevance continues to be debated ⁵. In
53 fact, the effects detected by biomarkers and individual responses can be directly related to the
54 presence of contaminants but do not inform on the severity of environmental quality
55 degradation in terms of ecological effects, because they cannot be directly interpreted as
56 predictors of the impacts on populations or communities, which constitute the protection
57 goals of ecosystem management. One promising way to overcome this difficulty is to include
58 the impacts measured on individual demographic parameters (*e.g.* survival, growth,
59 reproduction) in population models to investigate adverse outcomes at the population level ⁶⁻⁸.
60 Nevertheless, although such population models are currently increasingly used in predictive
61 approaches ⁹, their use in the diagnostic framework remains limited. In the majority of
62 studies, population models are based on laboratory data with species that are not
63 representative of ecosystems. Consequently, while these models are useful for extrapolating
64 the effects of a specific toxicant observed during a laboratory experiment on a model species
65 to outcomes on the population growth rate for instance ^{7, 10}, the integration of field-based
66 input data in modelling approaches is lacking to really anticipate what would happen in the

67 field in native populations ^{11, 12}. Therefore, to develop the use of population models as
68 predictive tools, we need to develop models based on field data and autochthonous species.

69 In the present study, we aimed to develop an ecologically relevant population model for the
70 crustacean *Gammarus fossarum*. Gammarids are recognized as tractable organisms for water
71 quality biomonitoring ^{6, 13}. We have recently contributed to the development of several sub-
72 individual biomarkers ¹⁴⁻¹⁷ and individual markers ^{4, 18} for this sentinel species. Gammarids
73 are considered as very promising species for multi-level assessment schemes from sub-
74 individual to population or community levels ⁶. Here, in a first step, we report the
75 implementation of a population modelling approach suited for the life-history and phenology
76 of this invertebrate species. We parameterized a periodic matrix population model ^{12, 19, 20}
77 based on a 1-year study of a perennial population of *G. fossarum*. We used a combination of
78 laboratory and *in situ* experiments in order to precisely characterize life-history trait dynamics
79 throughout the year. This model allowed us to capture the population dynamics and to
80 understand the particular pattern of demographic sensitivities in *Gammarus*, *e.g.* the relative
81 importance of recruitment processes (fertility) *vs* survival processes, or the temporal
82 variability of population vulnerability. In a second step, we demonstrate the suitability of this
83 population model for a multi-level assessment of water quality based on a case study on the
84 Amous watershed, a French river known to be contaminated by heavy metals due to mine
85 drainage. Finally, we discuss the potential contribution of this type of population modelling
86 approach to environmental monitoring, considering that biomarkers and individual responses
87 could be complemented by population models to decipher the role of environmental
88 contamination toxicity in ecological perturbations.

89

90 **2. MATERIALS AND METHODS**

91 **Biological data**

92 We conducted our experiments on a long-established population of *Gammarus fossarum*
93 which is present all the year upstream of the Ardières River (04°31'16 E; 46°11'12 N, Rhône,
94 France). We used a dual approach combining laboratory and field experiments to characterize
95 life-history trait variability throughout the year and population dynamics. On the one hand,
96 we conducted a field-based demographic sampling based on a monthly population census to
97 estimate population characteristics (*e.g.* changes in density and size structure, fertility). On the
98 other hand, we quantified the influence of water temperature throughout the year on the
99 growth rate and interlaying interval, by coupling laboratory experiments and *in situ*
100 validation. For all experiments, water temperature was recorded every 2 h using the Tinytag
101 temperature logger Aquatic 2 ®.

102

103 *Field-based demographic sampling*

104 A demographic sampling was conducted from November 2008 to November 2009. Each
105 month, gammarids were sampled along a 50-m river section using a hand net (25 × 18 cm).
106 Separate samples were taken for each substrate in the river, including favourable substrates
107 for gammarids (*i.e.* bryophytes, leaves) and dominant substrates in the river (*i.e.* gravels). The
108 percentage of each substratum was estimated on six transects shared out along the station.
109 Samples were sieved on site at 1.25 mm to separate juveniles from adults. Juveniles were
110 fixed in alcohol and adults were placed in buckets with river water. Juvenile densities were
111 estimated within the different substrates with a sub-sample corresponding to 20% of the total
112 sample from which we measured the body size of 60 individuals. For this measurement, we
113 used the length of the second segment of the antenna, which proved to be a robust indicator of
114 the body size in juveniles, adult males and females (data not shown). Concerning adults, we
115 counted gammarids within the different substrates and separated *in vivo* gravid females. Then
116 the body size of 60 individuals from the sample of gravid females was measured, and 60

117 individuals from the sample of males and non-gravid females were sexed using a binocular
118 microscope and measured. This methodology allowed us to estimate monthly population
119 density, size distribution, sex ratio and percentage of gravid females. By this means, we also
120 determined size at birth, size at maturity and maximum size. In addition, every month we
121 measured size and fertility (number of embryos in the marsupium) on 60 gravid females
122 covering a wide range of sizes sampled randomly in the river section. The detailed fertility
123 measurement procedure is described in Geffard et al. ¹⁸.

124

125 *Quantification of the monthly variability in growth rates and interlaying intervals*

126 Water temperature is known to influence the life-history traits of gammarids ²¹⁻²⁵.
127 Therefore, we expected that the variability in growth rates and interlaying intervals would be
128 mainly explained by water temperature variability during the year. Consequently, in the first
129 step we studied the influence of water temperature on growth and interlaying interval under
130 laboratory conditions. In the second step, we confirmed predictions using *in situ* caging
131 assays.

132 *Laboratory experiments.* To estimate the influence of temperature on growth, we tested
133 three temperatures, 7.0 (\pm 0.05), 12.1 (\pm 0.01) and 16.4 (\pm 0.03) °C, as representative of the
134 range observed at the study site (mean monthly water temperature varied from 5.2 to 15.9°C
135 in the year of the study). Because the growth was slow (in particular for low water
136 temperatures), we decided not to investigate growth from neonates to adults but to observe the
137 growth of three size classes of organisms simultaneously: 2.5 (\pm 0.3) mm, 4.5 (\pm 0.8) mm and
138 5.8 (\pm 0.7) mm. It allowed us to estimate growth from juveniles to adults using relatively
139 short experiments which is an advantage when studying gammarids under laboratory (*e.g.* no
140 nutrient deficiencies, less mortality). Gammarids were exposed to the three temperatures for
141 56 days. We used four replicates of 15 individuals for the first size class and four replicates of

142 10 individuals for the other two. Gammarids were placed in 0.5-L beakers filled with
143 continuously renewed water (four renewals per day; hardness 88 mg L⁻¹ of CaCO₃
144 corresponding to the hardness of the river at the study site). A pumping system maintained
145 oxygen in the beakers and a 16 h / 8 h light / dark photoperiod was applied. The organisms
146 were fed *ad libitum* with alder leaves conditioned in groundwater. Twice a week, freeze-dried
147 worms (*Tubifex*) were added. For the first size class, we also added frozen faeces from adult
148 batches. The body size of individuals was measured at days 0, 14, 32, 46 and 56. After having
149 tested different classes of non-linear growth models, we chose to fit experimental data with a
150 logistic model. For each temperature, a logistic model was thus fit simultaneously considering
151 the three classes of gammarids. The model is expressed as follows:

$$152 \quad L(t) = \frac{L_{max}}{1 + \left(\frac{L_{max}}{L_{init}} - 1 \right) e^{(-rt)}} \quad (1)$$

153 where $L(t)$ corresponds to the size of gammarids at time t (in days), L_{max} to the
154 maximum size, L_{init} to the size at the beginning of the experiment and r to the daily growth
155 rates of the logistic model. Considering 99% percentiles in total size distributions of the field-
156 based demographic sampling (see below), we set L_{max} at 8.5 mm. For the quantification of
157 interlaying intervals, because laying is synchronous with moult in gammarids^{16, 18, 26}, we used
158 the relationship established in a study on moulting dynamics (unpublished data). From this,
159 the influence of temperature θ (in °C) on the interlaying interval d (in days) is described by:

$$160 \quad d = \frac{(30.61 - 0.39 \theta)}{(0.01 + 0.05 \theta)} \quad (2)$$

161 This hyperbolic relationship is consistent with studies reported for *Gammarus*^{22, 27}.

162 *In situ* assays. We tested the predictive ability of these models of temperature influence on
163 growth rates and interlaying intervals during four campaigns of *in situ* caging experiments at
164 different seasons between November 2008 and November 2009 (*i.e.*, November-December

165 2008 for winter caging; April 2009 for spring; June 2009 for summer and October 2009 for
166 autumn). Mean water temperature during *in situ* experiments was ranged from 7.8 to 15.1°C.
167 The gammarids were sampled and calibrated (*i.e.* selection of homogenous size) directly at
168 the study site. To determine growth rates, depending on the availability of gammarids, we
169 used from one to three size classes. For each size class, three replicates of 12 organisms were
170 placed in cylinders capped at their ends with pieces of netting (mesh size, 350 µm). Alder
171 leaves were supplied *ad libitum*. Initial sizes were estimated with a sample of 30 organisms.
172 After one month of exposure, gammarids were counted for survival estimation, placed in
173 alcohol and measured. Concerning the interlaying interval, we adapted the protocol proposed
174 in Geffard et al.¹⁸. Three replicates of seven pre-copulatory pairs of gammarids (*i.e.* male and
175 female on amplexus, with the female at the end of its reproductive cycle) were placed in
176 cylinders (diameter, 5 cm; length, 10 cm) capped at their ends with pieces of netting (mesh
177 size, 1 mm). Alder leaves were supplied *ad libitum*. Every 2 days, gammarids were checked
178 in order to record the dates of moults (*i.e.* a first moult which occurred a few days after the
179 beginning of the experiment and a second which depended on temperature (between 4 and 8
180 weeks).

181

182 **Modelling framework and demographic analysis**

183 *Development of the population model*

184 We used a periodic Lefkovitch matrix population model with five size classes^{19, 20, 28, 29}
185 with the same structure as the model we previously developed for the gastropod
186 *Potamopyrgus*¹². We employed a size-class rather than an age-class or a stage-class model
187 because (*i*) a strong correlation exists between body size and life-history traits in gammarids
188^{22, 25, 27} and (*ii*) the life-history of individuals of such birth flow populations from short-living
189 species inhabiting variable environments (seasonality) strongly depends on their date of birth

190 in the year, which makes age a very weak predictor of biological features. The present model
 191 only deals with females and distinguishes two classes of juveniles – J1 (individuals with a
 192 size up to 3.5 mm) and J2 (size from 3.5 mm to the size at maturity) – and three classes of
 193 adults – A1 (from the size at maturity to 6 mm), A2 (from 6 to 7 mm) and A3 (greater than 7
 194 mm). This model can therefore integrate heterogeneity of demographic rates (survival, growth
 195 and fertility) between size classes throughout the year.

196 Let $n_i(k)$ be the number of individuals of size class i ($i = 1$ for J1, $i = 2$ for J2, $i = 3$ for A1, i
 197 $= 4$ for A2 and $i = 5$ for A3) at the beginning of month k . The five $n_i(k)$ variables can be
 198 gathered in a population vector $\mathbf{n}(k)$. Then we can define 12 monthly matrices \mathbf{M}_k , which link
 199 the population vectors $\mathbf{n}(k)$ between months k and $k+1$ as follows:

$$200 \quad \mathbf{n}(k+1) = \mathbf{M}_k \mathbf{n}(k) \quad (3)$$

201 with:

$$202 \quad \mathbf{M}_k = \begin{bmatrix} s_1(k) \left(1 - \sum_{j>1} g_{1,j}(k) \right) & 0 & f_3(k) \sqrt{s_1(k)} \sqrt{s_3(k)} & f_4(k) \sqrt{s_1(k)} \sqrt{s_4(k)} & f_5(k) \sqrt{s_1(k)} \sqrt{s_5(k)} \\ s_1(k) g_{1,2}(k) & s_2(k) \left(1 - \sum_{j>2} g_{2,j}(k) \right) & 0 & 0 & 0 \\ s_1(k) g_{1,3}(k) & s_2(k) g_{2,3}(k) & s_3(k) \left(1 - \sum_{j>3} g_{3,j}(k) \right) & 0 & 0 \\ s_1(k) g_{1,4}(k) & s_2(k) g_{2,4}(k) & s_3(k) g_{3,4}(k) & s_4(k) (1 - g_{4,5}(k)) & 0 \\ s_1(k) g_{1,5}(k) & s_2(k) g_{2,5}(k) & s_3(k) g_{3,5}(k) & s_4(k) g_{4,5}(k) & s_5(k) \end{bmatrix} \quad (4)$$

203 where $s_i(k)$ is the survival rate (proportion) of the size class i during month k , $g_{i,j}(k)$ the
 204 transition rate (proportion) between size classes i and j during month k , and $f_i(k)$ the
 205 reproductive rate (mean number of juveniles produced per individual) of the size class i
 206 during month k . The product of the 12 monthly matrices \mathbf{M}_k leads to an annual periodic
 207 matrix \mathbf{L} , which links the population vector from year t to year $t+1$ as follows:
 208

$$209 \quad \mathbf{n}(t+1) = \left(\prod_{k=1}^{12} \mathbf{M}_k \right) \mathbf{n}(t) = \mathbf{L} \mathbf{n}(t) \quad (5)$$

210

211 *Parameter estimation*

212 This matrix model encompasses three types of elements corresponding to survival,
213 reproductive and transition rates (see Coulaud et al. ¹²). For each month k , we estimated the
214 parameters from our laboratory and field experiments. We estimated the reproductive rates
215 $f_i(k)$ of the three adult classes ($i = 3, 4$ or 5) as follows:

$$216 \quad f_i(k) = \frac{sr_i(k) b_i(k) \rho_i(k) \Delta t(k)}{d(k)} \quad (6)$$

217 where $sr_i(k)$ (proportion of females) corresponds to the sex ratio of class i during month k ,
218 $b_i(k)$ to fertility (mean number of embryos carried by gravid female) of class i during month
219 k , $\rho_i(k)$ to the percentage of gravid females (proportion) in class i during month k , $\Delta t(k)$ to
220 the number of days of month k and $d_i(k)$ to the interlaying interval in days computed for
221 month k . Parameters $sr_i(k)$ and $\rho_i(k)$ were obtained with data from the demographic
222 sampling (see above); parameters $b_i(k)$ were estimated for each size class from the
223 relationship between body size (mm) and fertility (number of embryos) obtained from the
224 demographic sampling and parameters $d(k)$ were calculated according to eq. 2 with the mean
225 monthly water temperatures ($^{\circ}\text{C}$). We calculated transition rates $g_{i,j}(k)$ (proportion of
226 individuals from size class i reaching a size embedded in class j) using the relationship
227 between growth rate (day^{-1}) and water temperature ($^{\circ}\text{C}$) (eq. 1) established during the
228 laboratory experiment and validated during *in situ* caging experiment (see above). Lastly, we
229 estimated survival rates $s_i(k)$ for month k from the comparison of densities (gammarid.m^{-2})
230 observed during the demographic sampling (see above) in month k with densities expected
231 from the observed densities in month $k-1$ combined with growth and reproductive rates
232 estimated for month $k-1$.

233

234 *Model outcomes and elasticity analysis*

235 The first dominant eigenvalue of the Lefkovich matrix \mathbf{L} , λ , corresponds to the asymptotic
236 growth rate of the gammarid population²⁸. The right eigenvector w associated with this first
237 eigenvalue gives the asymptotic stable size structure. According to the matrix used first in the
238 product of the 12 monthly matrices \mathbf{M}_k , we obtained the size structure at the end of each
239 month of the year. Elasticities were calculated through the reduction in the asymptotic
240 population growth rate λ induced by 10% reduction on all monthly matrices \mathbf{M}_k in each life-
241 history trait successively and independently (*i.e.* survival of each class, fertility, reproductive
242 cycle duration and growth) before the calculation of the matrix \mathbf{L} . We also examined the
243 monthly variability of this elasticity pattern. For this, we applied an episodic but more severe
244 50 % reduction in juvenile survival (s_1 and s_2), adult survival (s_3 , s_4 and s_5) and fertility
245 successively and independently on only one monthly matrix \mathbf{M}_k before the calculation of the
246 matrix \mathbf{L} .

247

248 **Case study on the Amous watershed**

249 Following the transplantation methodology developed in our group¹⁴⁻¹⁷, a campaign of *in*
250 *situ* assays was conducted in March 2008 in four stations of the Amous watershed, a French
251 river known to be contaminated by heavy metals originating from mine drainage from the
252 former mine at Carnoulès^{4, 30}. The same four stations as in these two previous studies were
253 considered: three stations along the Amous River: *Upstream -1500 m*, *Downstream +1200 m*
254 and *Downstream +3500 m* with different levels of metallic contamination (*i.e.*, *Upstream*
255 *-1500 m < Downstream +3500 m < Downstream +1200 m*, for metal bioaccumulation data
256³⁰), and a fourth reference station on a tributary from the same river system (*Tributary*) that is
257 not impacted by metal-loaded mine leachates. Juvenile survival, adult survival and fertility

258 were measured in the different stations. We used gammarids from a station displaying good
259 water quality and currently used by our laboratory for *in situ* assays¹⁴⁻¹⁷ located upstream of
260 the Bourbre River. To estimate juvenile survival, four replicates of 12 individuals were placed
261 in cylinders capped at their ends with pieces of netting (mesh size, 350 μm). For adult
262 survival and fertility, three replicates of seven pre-copulatory pairs were placed in cylinders
263 (mesh size, 1 mm). Gammarids were exposed for 21 days and were fed *ad libitum* with alder
264 leaves. At the end of exposure, gammarids were counted and fertility was measured (*i.e.*
265 number of embryos in the marsupium). To estimate population impacts, we integrated these
266 different individual impacts into our population model in terms of percentage of demographic
267 rate reduction in comparison to the control levels observed in the reference station *Tributary*.

268

269 **Statistical analyses**

270 Statistical procedures and population models were implemented with the R software³¹.
271 Before performing the ANOVA procedure, normality and homoscedasticity were checked
272 using the Shapiro-Wilk and Bartlett tests.

273

274 **3. RESULTS**

275 **Field-based demographic sampling: size structure and fertility**

276 Changes of size distribution in the population, as estimated with the monthly field-based
277 demographic sampling, are presented in Figure S1. The highest densities were observed in
278 autumn and at the beginning of winter, while the lowest densities were observed in winter and
279 spring. We observed highly fluctuating densities of juveniles, with very low densities in
280 spring and high densities during the rest of the year, particularly autumn. Contrasting with
281 juveniles, adults are present throughout the year with little variability and persist during
282 winter. Considering 1% and 99% percentiles in total size distributions, we estimated a size at

283 birth equal to 2.3 (\pm 0.2) mm and a maximum size equal to 8.2 (\pm 0.3) mm. Considering 1%
284 percentiles of reproductive female size distributions, we estimated a size at maturity equal to
285 5.2 (\pm 0.3) mm. These values appeared constant during the year. The monthly demographic
286 sampling allowed us to estimate the percentage of females in reproduction $\rho_i(k)$ and the sex
287 ratio $sr_i(k)$. We observed substantial between-month and between-class variability of $\rho_i(k)$
288 values (from 0.1 to 95%). For all months, we observed an increase in this percentage between
289 the three size classes. Furthermore, we noted low percentages of reproductive females at the
290 end of autumn and during winter, as well as high percentages during spring and summer. For
291 sex ratio $sr_i(k)$, we generally observed an equal number of males and females. Consequently,
292 we set the sex ratio at 0.5 in the model. A strong positive relationship was detected between
293 body size and fertility without seasonal influence (Figure S2). Size class A1 females had a
294 mean fertility of 3.6 (\pm 1.3) embryos, A2 females a mean fertility of 5.1 (\pm 1.6), and A3
295 females a mean fertility of 9.2 (\pm 2.9) embryos.

296

297 **Monthly variability of growth rates and interlaying intervals**

298 The measurements taken during the laboratory experiment on growth are presented on
299 Figure S3 (A, B, C), showing that individuals grew faster when temperature increased. With
300 the logistic models fitted simultaneously on the three size classes (Figure S3 A, B, C), we
301 estimated daily growth rates for each temperature. Between 7.0 and 16.4°C, they varied from
302 0.008 to 0.021 day⁻¹. In this temperature range, consistent with temperatures recorded at the
303 study site during the year, we fitted a linear model between water temperature θ (in °C) and
304 daily growth rate r (day⁻¹):

$$305 \quad r(\theta) = 0.0014 \theta - 0.0024 \quad (4)$$

306 During the *in situ* assays performed at different seasons, we observed substantial variability
307 in daily gain in size (*i.e.*, between 0.011 and 0.052 mm.day⁻¹ depending on the season and the

308 size-class). When the observed sizes were compared for each size class with values predicted
309 from the logistic model established in laboratory exposure (eq. 1) combined with (eq. 4), we
310 observed a good correlation (Spearman rank correlation test, $p < 0.05$, $r^2 = 0.87$) (Figure S3
311 D), which validates the fact that this variability in growth rates is mainly related to water
312 temperature variability between the different caging experiments.

313 During the *in situ* experiments, we recorded an interlaying interval of 34 days in spring and
314 26 days in summer. These values are consistent with model predictions from eq. 2, which
315 predicts durations of 35.5 and 27.1 days, respectively. During winter and autumn, we were
316 not able to follow females up to the end of the reproductive cycle due to the low temperature
317 which induces long reproductive cycles.

318

319 **Population model analysis**

320 Regarding parameter estimation (Table S1), we observed considerable monthly and
321 between-class variability in reproductive rates $f_i(k)$, which varied from 0.01 to 7.07 in the
322 mean number of juveniles produced per month per female. Concerning transition rates $g_{i,j}(k)$,
323 we also observed high monthly variability, with a majority of individuals staying in their
324 initial size class during the coldest months, whereas during months with a high water
325 temperature, a majority of individuals moved up one or two size classes from month to
326 month. Computed adult survival rates show substantial seasonal variability with low survival
327 rates in summer, whereas survival rates were high in winter and spring. Furthermore, size
328 class A3 showed the lowest survival rates for all months. Juvenile survival rates were
329 generally higher than adult survival rates. For some months, we calculated survival rates
330 higher than 1, in particular when densities were low (*i.e.* the uncertainty in count estimates
331 increased with smaller size samples) or for size class J1 (*i.e.* gammarids of the size class J1
332 were very small and therefore difficult to sample, which makes density estimation difficult).

333 To generate a more robust estimation of survival rates for each month k to implement the
334 population model, we used the same smoothing methodology as in our study on the mollusc
335 *Potamopyrgus*¹². We calculated the geometric mean of the survival rate estimates for months
336 $k-1$, k and $k+1$.

337 The asymptotic population growth rate λ was estimated at 1.07. We computed the stable
338 size distribution corresponding to the structure of the population at the end of November,
339 February, May and August (Figure 1). We observed good consistency with field data of the
340 demographic sampling (chi-square tests not significant for the four seasons). The elasticity
341 analysis on matrix L (Figure 2) highlights that the asymptotic population growth rate λ is
342 more sensitive to relative changes in juvenile survival rates than to changes in the other life-
343 history parameters. The life-history traits corresponding to the second highest elasticity are
344 the survival rates of small adults (*i.e.* elasticities of s_3 and s_4), followed by fertility (b),
345 interlaying interval (d), growth rate (r) and survival rate of larger adults (s_3). Although the
346 population is generally more sensitive to impacts on juvenile survival, when we applied 50%
347 reductions in juvenile survival, adult survival or fertility rates successively on each monthly
348 matrix M_k , we observed a strong variability of population sensitivity throughout the year
349 (Figure 3). Reduction in juvenile survival rates led to the highest impacts in June, then in
350 autumn. Concerning adult survival, we noted the highest impacts in winter with more than
351 20% reduction in λ when survival reduction occurred in January, February or March. Finally,
352 concerning fertility, we observed a bimodal pattern with the highest impacts in April and in
353 July-August.

354

355 **Case study on the Amous watershed**

356 In comparison to the reference station *Tributary*, we observed impacts on juvenile survival
357 rates (s_j) in *Upstream -1500 m* and *Downstream +1200 m* (unilateral proportion test, $p <$

358 0.05), on adult survival rates (s_a) in *Downstream +1200 m* (unilateral proportion test, $p <$
359 0.05) and on fertility (b) in *Upstream -1500m* and *Downstream +3500 m* (Wilcoxon rank
360 sum test, $p < 0.05$) (Table 1 A). In *Downstream +1200 m*, we did not record fertility due to
361 excessively high adult mortality. When we applied simultaneously the effects in term of
362 percentage of reduction in comparison to the reference site *Tributary* on all monthly matrices
363 \mathbf{M}_k before the calculation of the matrix \mathbf{L} , we predicted severe impacts on the asymptotic
364 population growth rate in all contaminated stations (Table 1 B, Table S2). We also calculated
365 the specific impacts of the degradation of each life-history trait (Table 1 B, Table S2) with a
366 one-by-one application of the effects on each life-history-trait in term of percentage of
367 reduction in comparison to the reference site *Tributary*. In this way, we noted that in
368 *Upstream -1500 m* impacts on fertility were responsible for the great majority of global
369 impacts on population dynamics, whereas in *Downstream +1200 m*, reduction in juvenile
370 survival rates had the greatest impact at the population level.

371

372 4. DISCUSSION

373 **Picturing the *G. fossarum* population biology in the field**

374 We have described the characteristics of one population of *G. fossarum* by means of a
375 combination of a field survey and laboratory or *in situ* experiments. During the field-based
376 demographic sampling, we observed fluctuating densities throughout the year (Figure S1)
377 with high-density peaks (*i.e.* more than 800 gammarids per m^2 in September and December)
378 and periods of lower densities, in particular at the end of winter and at the beginning of spring
379 . This high seasonal variability in gammarid density agrees with other studies on *G. fossarum*
380 ³²⁻³⁴. Our population is mainly composed of juveniles, except in spring where adults are more
381 abundant, agreeing with previous data ³². In this way, the persistence of the population at the
382 beginning of spring when densities are minimal is ensured by the survival of an overwintering

383 stock of adults. As for the percentage of reproductive females, we observed significant
384 between-month variability with a high percentage in summer and a very low percentage in
385 winter. This pattern is consistent with other studies on *G. fossarum*³² or other gammarid
386 species^{35, 36}, which report a higher reproductive activity in warm seasons. The estimation of
387 the seasonal variability of life-history traits confirmed our primary hypothesis that
388 temperature is the main source of variability. This is consistent with previous
389 ecophysiological studies, which have shown that daily growth rates^{22, 25, 27, 37} and interlaying
390 intervals^{23, 38-40} are mainly modulated by temperature. Density-dependent processes could
391 also be involved in temporal patterns of survival, and they could further be taken into account
392 with an appropriate amendment of our model. But we should dispose from a multi-year
393 demographic monitoring (ongoing study), to decipher whether such effects occur here in
394 *Gammarus* population dynamics.

395 Nevertheless, this complex population dynamics in a natural freshwater environment is well
396 described by the different outcomes of our population model. Indeed, from the analysis of the
397 annual matrix model, a good match was found between the stable size distribution computed
398 for each season and the population structure observed during the field demographic sampling
399 (Figure 1). This highlights that the present modelling approach succeeds in properly
400 describing the dynamics of this *G. fossarum* population throughout the year. It confirms that
401 periodic matrix population models with size classes can be very useful tools to capture the
402 dynamics of such small invertebrate species¹². We showed that the population dynamics is
403 particularly vulnerable to juvenile mortality (Figure 2). This high sensitivity to juvenile
404 survival reduction is consistent with a study on the estuarine amphipod *Leptocheirus*
405 *plumulosus*⁴¹. More generally, it also agrees with Forbes et al.⁴², who concluded that benthic
406 macro-invertebrate species generally show a high sensitivity to reduction on juvenile survival
407 rates.

408 In addition, the sensitivity of the *Gammarus* population studied varies substantially between
409 months (Figure 3). For instance, the population dynamics appeared highly sensitive to adult
410 survival reductions in winter, whereas it is more sensitive to fertility inhibitions in April, July
411 and August. McGee and Spencer^{41, 43} also concluded in high monthly variability of
412 population sensitivity, but the monthly sensitivity pattern was different in *L. plumulosus*.
413 These contrasting patterns highlight the role of species life-histories in governing
414 demographic impacts. The pattern of demographic sensitivity in *G. fossarum* is consistent
415 with our understanding of its population biology. We observed a functioning of the population
416 with two renewal time periods in the year. In spring, an overwintering stock of adults
417 provides the main contributors to population renewal, and this explains the high sensitivity to
418 the adult survival rate in winter and a peak of fertility sensitivity in April (Figure 3). The
419 juveniles produced by these surviving breeders in early spring reach maturity in summer and
420 in turn contribute to the production of new individuals in the population. This results in a
421 second peak of sensitivity to fertility inhibitions in July and August, preceded by a peak of
422 sensitivity to juvenile survival rate reductions in April and May. Thereafter, high sensitivity to
423 juvenile survival reduction appears during autumn, because the survivors from this second
424 wave of new individuals constitute the overwintering stock of adults, which mainly ensures
425 the population restarting in the next year. The modelling approach developed in this study is
426 thus suitable to mechanistically understand the complexity of the demographic processes
427 occurring in a wild *G. fossarum* population. Therefore, this approach can be used to anticipate
428 population impacts of life-history trait alterations caused by toxic environmental
429 contaminations, taking into account the influence of life-history and phenology for this effect
430 upscaling at the population level. On a methodological point, our modelling approach would
431 be fully complemented with the challenging possibility to adapt in the present case of a birth

432 flow population, the analytical methodology of sensitivity analysis developed for periodic
433 matrix models²⁰.

434

435 **Application to improve the ecological relevance of water quality diagnostic**

436 Combining active biomonitoring approaches and population modelling is a promising way
437 to perform an ecologically relevant assessment at the population level for diagnostic purposes
438 ⁶. On the one hand, the biomonitoring methodology of *in situ* caging makes it possible to
439 measure the impact of toxicants on the life-history traits of native species in the field⁴⁴. On
440 the other hand, population models, which are recognized as relevant tools for projecting
441 individual effects to consequences on population dynamics⁶⁻⁸, provide an assessment at an
442 ecologically relevant level of biological organization. We have illustrated this approach herein
443 with the Amous watershed study. At the three contaminated stations, we observed impacts on
444 life-history traits on caged gammarids (Table 1). When introducing these alterations of life-
445 history traits in the population model, in all cases we anticipated severe consequences on the
446 asymptotic population growth rate λ (between 80 and 99% reduction, Table 1). Interestingly,
447 we also separately considered the potential reduction in λ of the impacts observed on the
448 different life-history traits. Thereby, in comparison with the reference station *Tributary*, we
449 observed that a 15% reduction in the juvenile survival rate (*i.e.* in the station *Upstream -1500*
450 *m*) impacts λ with the same severity as a 56% reduction in the adult survival rate (*i.e.* in the
451 station *Downstream +1200 m*) or a 58% reduction in fertility (*i.e.* in the station *Downstream*
452 *+3500 m*). This pattern is explained by the greater sensitivity of population dynamics to
453 impacts on juvenile survival as revealed by the model's elasticity analysis. Of note,
454 accrediting the relevance of the model predictions, a natural gammarid population is present
455 all along the year in the station *Tributary*, while no gammarids can be harvested in the two
456 contaminated *Downstream* stations. In the station *Upstream -1500m*, gammarids can be found

457 episodically, but these are mainly adults, with high occurrence of necrotic gills; no embryos
458 are present in females, and juvenile density is quite null. These observations indicate that
459 organisms present in this station do not constitute a durable population, but are rather drifting
460 animals from more upstream pristine areas.

461 Furthermore, this modelling approach with periodic matrix population models has particular
462 value for the diagnostic of water quality. Indeed, in addition to characterizing the impact of
463 toxicants in persistent chronic pollution contexts, the periodic structure of these models can
464 anticipate the impact of pulsed sources of contamination, such as peaks of pesticides or
465 contaminations with seasonal variability due to water flow, run-off or effluent emission
466 management. This is in fact particularly relevant with regard to significant between-month
467 differences in population vulnerability (Figure 3). Thus the development of population models
468 that integrate seasonality is a relevant way to increase our ability to project toxic effects on
469 individual performance onto population demographic consequences. One question still to be
470 resolved is how much between-population and between-species variability of life-history
471 phenology could condition the relevance of the approach, which presumed a genericity of
472 demographic patterns in *Gammarids*.

473 Finally, this study contributes to establishing gammarids as sentinel species for European
474 freshwater ecosystems^{6, 13}. Indeed, we have already mentioned that numerous biomarkers
475 tracking toxic effects at the molecular level and *in situ* bioassay protocols are available in
476 these species. Here we demonstrate how alterations of life-history traits could be translated in
477 terms of potential population impacts, by means of an ecologically relevant population model.
478 Therefore, gammarids are good candidates to elaborate multilevel assessment schemes for
479 environmental monitoring. Indeed, based on mechanistic hypotheses as proposed for the
480 predictive hazard assessment of chemical compounds⁴⁵⁻⁴⁷, one could establish quantitative
481 links between sub-individual biomarker responses and individual performance alterations⁴⁸⁻

482 ⁵⁰, and then use population modelling. In the context of environmental management, this
483 could allow combining the sensitivity and the specificity of field ecotoxicological tools with
484 the ecological relevance of a diagnostic of toxicity projected at the population level.

485

486 **ASSOCIATED CONTENT**

487 **Supporting Information**

488 Supporting information provides details on biological data measurement allowing the
489 parameterization of the population model. Figure S1 relates monthly field-based demographic
490 sampling data, Figure S2 relates details on the relationship between body size and female
491 fertility, and Figure S3 relates details on growth experiments. Table S1 gives the different
492 parameters of the population model (reproductive rates, transition rates and survival rates) and
493 Table S2 gives the actual lambda values corresponding to the Table 1 B. This material is
494 available free of charge via the Internet at <http://pubs.acs.org>.

495

496 **AUTHOR INFORMATION**

497 **Corresponding Author**

498 *Phone: 33 4 72208788. Fax: 33 4 78477875. E-mail: arnaud.chaumot@irstea.fr.

499 Corresponding author address: Irstea, UR MALY, 5 rue de la doua – CS70077, F-69626
500 Villeurbanne, France.

501 **Note**

502 The authors declare no competing financial interest.

503

504 **ACKNOWLEDGMENTS**

505 The authors thank the Cluster Environnement of the Région Rhône-Alpes (France) for
506 financial grants, and the ANR CESA program GAMMA 021 02 “Variability-adaptation-
507 diversity and Ecotoxicology in gammarids” (2012-2015).

508

509 REFERENCES

510 1. Chapman, P. M., Determining when contamination is pollution - Weight of evidence
511 determinations for sediments and effluents. *Environ. Int.* **2007**, *33*, (4), 492-501.

512 2. Dagnino, A.; Sforzini, S.; Dondero, F.; Fenoglio, S.; Bona, E.; Jensen, J.; Viarengo,
513 A., A "Weight-of-Evidence" approach for the integration of environmental "Triad" data to
514 assess ecological risk and biological vulnerability. *Integr. Environ. Assess. Manage.* **2008**, *4*,
515 (3), 314-326.

516 3. Damásio, J.; Tauler, R.; Teixidó, E.; Rieradevall, M.; Prat, N.; Riva, M. C.; Soares, A.
517 M. V. M.; Barata, C., Combined use of *Daphnia magna* in situ bioassays, biomarkers and
518 biological indices to diagnose and identify environmental pressures on invertebrate
519 communities in two Mediterranean urbanized and industrialized rivers (NE Spain). *Aquat.*
520 *Toxicol.* **2008**, *87*, (4), 310-320.

521 4. Coulaud, R.; Geffard, O.; Xuereb, B.; Lacaze, E.; Quéau, H.; Garric, J.; Charles, S.;
522 Chaumot, A., In situ feeding assay with *Gammarus fossarum* (Crustacea): modelling the
523 influence of confounding factors to improve water quality biomonitoring. *Water Res.* **2011**,
524 *45*, 6417-6429.

525 5. Forbes, V. E.; Palmqvist, A.; Bach, L., The use and misuse of biomarkers in
526 ecotoxicology. *Environ. Toxicol. Chem.* **2006**, *25*, (1), 272-280.

- 527 6. Baird, D. J.; Brown, S. S.; Lagadic, L.; Liess, M.; Maltby, L.; Moreira-Santos, M.;
528 Schulz, R.; Scott, G. I., In situ-based effects measures: determining the ecological relevance
529 of measured responses. *Integr. Environ. Assess. Manage.* **2007**, *3*, (2), 259-267.
- 530 7. Forbes, V. E.; Calow, P.; Grimm, V.; Hayashi, T. I.; Jager, T.; Katholm, A.;
531 Palmqvist, A.; Pastorok, R.; Salvito, D.; Sibly, R.; Spromberg, J.; Stark, J.; Stillman, R. A.,
532 Adding value to ecological risk assessment with population modeling. *Hum. Ecol. Risk*
533 *Assess.* **2011**, *17*, (2), 287-299.
- 534 8. Forbes, V. E.; Calow, P., Extrapolation in Ecological Risk Assessment: Balancing
535 Pragmatism and Precaution in Chemical Controls Legislation. *Bioscience* **2002**, *52*, (3), 249-
536 257.
- 537 9. Galic, N.; Hommen, U.; Baveco, J. M.; Van Den Brink, P. J., Potential application of
538 population models in the european ecological risk assessment of chemicals II: Review of
539 models and their potential to address environmental protection aims. *Integr. Environ. Assess.*
540 *Manage.* **2010**, *6*, (3), 338-360.
- 541 10. Raimondo, S.; McKenney Jr, C. L., From organisms to populations: Modeling aquatic
542 toxicity data across two levels of biological organization. *Environ. Toxicol. Chem.* **2006**, *25*,
543 (2), 589-596.
- 544 11. Hansen, F.; Forbes, V. E.; Forbes, T. L., Using elasticity analysis of demographic
545 models to link toxicant effects on individuals to the population level: an example. *Funct.*
546 *Ecol.* **1999**, *13*, (2), 157-162.
- 547 12. Coulaud, R.; Mouthon, J.; Quéau, H.; Charles, S.; Chaumot, A., Life-history
548 phenology strongly influences population vulnerability to toxicants: A case study with the
549 mudsnail *Potamopyrgus antipodarum*. *Environ. Toxicol. Chem.* **2013**, *32*, (8), 1727-1736.

- 550 13. Kunz, P. Y.; Kienle, C.; Gerhardt, A., Gammarus spp. in aquatic ecotoxicology and
551 water quality assessment: Toward integrated multilevel tests. *Rev. Environ. Cont. Toxicol.*
552 **2010**, *205*, 1-76.
- 553 14. Xuereb, B.; Chaumot, A.; Mons, R.; Garric, J.; Geffard, O., Acetylcholinesterase
554 activity in Gammarus fossarum (Crustacea Amphipoda). Intrinsic variability, reference levels,
555 and a reliable tool for field surveys. *Aquat. Toxicol.* **2009**, *93*, (4), 225-233.
- 556 15. Lacaze, E.; Geffard, O.; Bony, S.; Devaux, A., Genotoxicity assessment in the
557 amphipod Gammarus fossarum by use of the alkaline Comet assay. *Mutat. Res.-Genet.*
558 *Toxicol. Environ. Mutag.* **2010**, *700*, (1-2), 32-38.
- 559 16. Jubeaux, G.; Simon, R.; Salvador, A.; Quéau, H.; Chaumot, A.; Geffard, O.,
560 Vitellogenin-like proteins in the freshwater amphipod Gammarus fossarum (Koch, 1835):
561 Functional characterization throughout reproductive process, potential for use as an indicator
562 of oocyte quality and endocrine disruption biomarker in males. *Aquat. Toxicol.* **2012**, *112-*
563 *113*, 72-82.
- 564 17. Charron, L.; Geffard, O.; Chaumot, A.; Coulaud, R.; Queau, H.; Geffard, A.;
565 Dedourge-Geffard, O., Effect of water quality and confounding factors on digestive enzyme
566 activities in Gammarus fossarum. *Environ. Sci. Pollut. Res.* **2013**, 1-13.
- 567 18. Geffard, O.; Xuereb, B.; Chaumot, A.; Geffard, A.; Biagiante, S.; Noël, C.; Abbaci,
568 K.; Garric, J.; Charmantier, G.; Charmantier-Daures, M., Ovarian cycle and embryonic
569 development in Gammarus fossarum: Application for reproductive toxicity assessment.
570 *Environ. Toxicol. Chem.* **2010**, *29*, (10), 2249-2259.
- 571 19. Caswell, H.; Trevisan, M. C., Sensitivity analysis of periodic matrix models. *Ecology*
572 **1994**, *75*, (5), 1299-1303.

- 573 20. Caswell, H.; Shyu, E., Sensitivity analysis of periodic matrix population models.
574 *Theor. Popul. Biol.* **2012**, *82*, (4), 329-339.
- 575 21. Pöckl, M.; Webb, B. W.; Sutcliffe, D. W., Life history and reproductive capacity of
576 *Gammarus fossarum* and *G. roeseli* (Crustacea: Amphipoda) under naturally fluctuating water
577 temperatures: A simulation study. *Freshwat. Biol.* **2003**, *48*, (1), 53-66.
- 578 22. Pöckl, M., Effects of temperature, age and body size on moulting and growth in the
579 freshwater amphipods *Gammarus fossarum* and *G. roeseli*. *Freshwat. Biol.* **1992**, *27*, (2), 211-
580 225.
- 581 23. Pöckl, M.; Timischl, W., Comparative study of mathematical models for the
582 relationship between water temperature and brood development time of *Gammarus fossarum*
583 and *G. roeseli* (Crustacea: Amphipoda). *Freshwat. Biol.* **1990**, *23*, (3), 433-440.
- 584 24. Sutcliffe, D. W.; Carrick, T. R.; Willoughby, L. G., Effects of diet, body size, age and
585 temperature on growth rates in the amphipod *Gammarus pulex*. *Freshwat. Biol.* **1981**, *11*, (2),
586 183-214.
- 587 25. Neuparth, T.; Costa, F. O.; Costa, M. H., Effects of temperature and salinity on life
588 history of the marine amphipod *Gammarus locusta*. Implications for ecotoxicological testing.
589 *Ecotoxicology* **2002**, *11*, (1), 61-73.
- 590 26. Hyne, R. V., Review of the reproductive biology of amphipods and their endocrine
591 regulation: Identification of mechanistic pathways for reproductive toxicants. *Environ.*
592 *Toxicol. Chem.* **2011**, *30*, (12), 2647-2657.
- 593 27. Pöckl, M., Laboratory studies on growth, feeding, moulting and mortality in the
594 freshwater amphipods *Gammarus fossarum* and *G. roeseli*. *Arch. Hydrobiol.* **1995**, *134*, (2),
595 223-253.

- 596 28. Caswell, H., *Matrix Population Models*. John Wiley & Sons, Ltd: 2001.
- 597 29. Lefkovitch, L. P., The study of population growth in organisms grouped by stages.
598 *Biometrics* **1965**, *21*, 1-18.
- 599 30. Dedourge-Geffard, O.; Palais, F.; Biagiante-Risbourg, S.; Geffard, O.; Geffard, A.,
600 Effects of metals on feeding rate and digestive enzymes in *Gammarus fossarum*: An in situ
601 experiment. *Chemosphere* **2009**, *77*, (11), 1569-1576.
- 602 31. R Development Core Team, *R: A Language and Environment for Statistical*
603 *Computing*. R Foundation for Statistical Computing: 2013.
- 604 32. Ladewig, V.; Jungmann, D.; Köhler, H. R.; Schirling, M.; Triebkorn, R.; Nagel, R.,
605 Population structure and dynamics of *Gammarus fossarum* (Amphipoda) upstream and
606 downstream from effluents of sewage treatment plants. *Arch. Environ. Contam. Toxicol.*
607 **2006**, *50*, (3), 370-383.
- 608 33. Beracko, P.; Sýkorová, A.; Štangler, A., Life history, secondary production and
609 population dynamics of *Gammarus fossarum* (Koch, 1836) in a constant temperature stream.
610 *Biologia* **2012**, *67*, (1), 164-171.
- 611 34. Welton, J. S., Life-history and production of the amphipod *Gammarus pulex* in a
612 Dorset chalk stream. *Freshwat. Biol.* **1979**, *9*, (3), 263-275.
- 613 35. Costa, F. O.; Costa, M. H., Life history of the amphipod *Gammarus locusta* in the
614 Sado estuary (Portugal). *Acta Oecol.* **1999**, *20*, (4), 305-314.
- 615 36. Sutcliffe, D. W., Reproduction in *Gammarus* (Crustacea, Amphipoda): female
616 strategies. *Freshwat. Forum* **1993**, *3*, (26-64).

- 617 37. Duran, M., Estimating the growth rate of *Gammarus pulex* (L.) from the River
618 Yeşilirmak (Turkey). *Arch. Hydrobiol.* **2004**, *161*, (4), 553-559.
- 619 38. Pöckl, M., Reproductive potential and lifetime potential fecundity of the freshwater
620 amphipods *Gammarus fossarum* and *G. roeseli* in Austrian streams and rivers. *Freshwat. Biol.*
621 **1993**, *30*, (1), 73-91.
- 622 39. Sutcliffe, D. W., Reproduction in *Gammarus* (Crustacea, Amphipoda): basic
623 processes. *Freshwat. Forum* **1992**, *2*, (102-128).
- 624 40. Maranhão, P.; Marques, J. C., The influence of temperature and salinity on the
625 duration of embryonic development, fecundity and growth of the amphipod *Echinogammarus*
626 *marinus* Leach (Gammaridae). *Acta Oecol.* **2003**, *24*, (1), 5-13.
- 627 41. McGee, B. L.; Spencer, M., A field-based population model for the sediment toxicity
628 test organism *Leptocheirus plumulosus*: II. Model application. *Mar. Environ. Res.* **2001**, *51*,
629 (4), 347-363.
- 630 42. Forbes, V. E.; Calow, P.; Sibly, R. M., Are current species extrapolation models a
631 good basis for ecological risk assessment? *Environ. Toxicol. Chem.* **2001**, *20*, (2), 442-447.
- 632 43. Spencer, M.; McGee, B. L., A field-based population model for the sediment toxicity
633 test organism *Leptocheirus plumulosus*: I. Model development. *Mar. Environ. Res.* **2001**, *51*,
634 (4), 327-345.
- 635 44. Liber, K.; Goodfellow, W.; den Besten, P.; Clements, W.; Galloway, T.; Gerhardt, A.;
636 Green, A.; Simpson, S., In situ-based effects measures: considerations for improving methods
637 and approaches. *Integr. Environ. Assess. Manage.* **2007**, *3*, (2), 246-258.

638 45. Kramer, V. J.; Etterson, M. A.; Hecker, M.; Murphy, C. A.; Roesijadi, G.; Spade, D.
639 J.; Spromberg, J. A.; Wang, M.; Ankley, G. T., Adverse outcome pathways and ecological
640 risk assessment: Bridging to population-level effects. *Environ. Toxicol. Chem.* **2011**, *30*, (1),
641 64-76.

642 46. Ankley, G. T.; Bennett, R. S.; Erickson, R. J.; Hoff, D. J.; Hornung, M. W.; Johnson,
643 R. D.; Mount, D. R.; Nichols, J. W.; Russom, C. L.; Schmieder, P. K.; Serrano, J. A.; Tietge,
644 J. E.; Villeneuve, D. L., Adverse outcome pathways: A conceptual framework to support
645 ecotoxicology research and risk assessment. *Environ. Toxicol. Chem.* **2010**, *29*, (3), 730-741.

646 47. Miller, D. H.; Jensen, K. M.; Villeneuve, D. L.; Kahl, M. D.; Makynen, E. A.; Durhan,
647 E. J.; Ankley, G. T., Linkage of biochemical responses to population-level effects: A case
648 study with vitellogenin in the fathead minnow (*Pimephales promelas*). *Environ. Toxicol.*
649 *Chem.* **2007**, *26*, (3), 521-527.

650 48. Jager, T.; Hansen, B. H., Linking survival and biomarker responses over time.
651 *Environ. Toxicol. Chem.* **2013**, *32*, (8), 1842-1845.

652 49. Lacaze, E.; Geffard, O.; Goyet, D.; Bony, S.; Devaux, A., Linking genotoxic
653 responses in *Gammarus fossarum* germ cells with reproduction impairment, using the Comet
654 assay. *Environ. Res.* **2011**, *111*, (5), 626-634.

655 50. Xuereb, B.; Lefèvre, E.; Garric, J.; Geffard, O., Acetylcholinesterase activity in
656 *Gammarus fossarum* (Crustacea Amphipoda): Linking AChE inhibition and behavioural
657 alteration. *Aquat. Toxicol.* **2009**, *94*, (2), 114-122.

658

659 **TABLES**

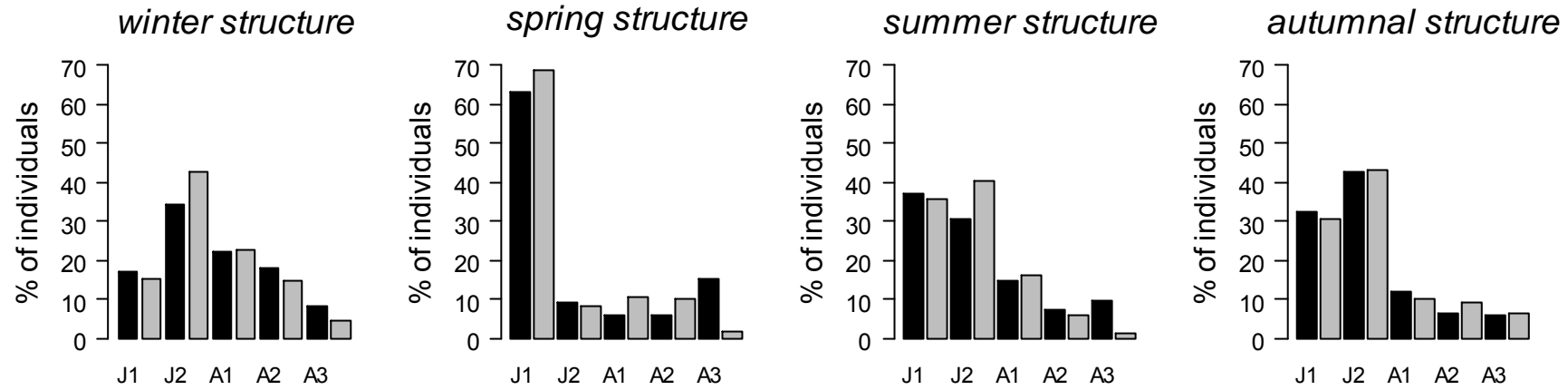
660 **Table 1. A)** Juvenile survival (%), adult survival (%) and fertility (embryos per females)
 661 values measured in the stations in the Amous watershed. * indicated significant inhibitions in
 662 comparison with the reference station Tributary. **B)** Percentage of inhibition of population
 663 growth rate λ caused by the different individual impacts observed in the three contaminated
 664 stations.

Stations				
	<i>Tributary</i>	<i>Upstream -1500 m</i>	<i>Downstream +1200 m</i>	<i>Downstream +3500 m</i>
A) Recorded individual traits during <i>in situ</i> assay				
juvenile survival (%)	83	71*	19*	95
adult survival (%)	96	92	42*	94
fertility (embryos per female)	18.0	1.7*	/	7.5*
B) Projected population impacts				
(% reduction in the asymptotic population growth rate λ)				
all traits	/	99	99	80
juvenile survival	/	65	99	no impact
adult survival	/	no impact	81	no impact
fertility	/	98	/	80

665

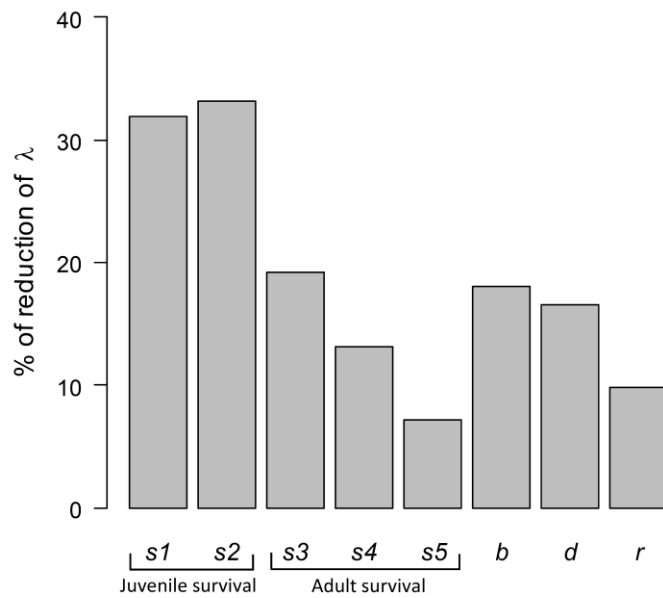
666

667 **FIGURES**



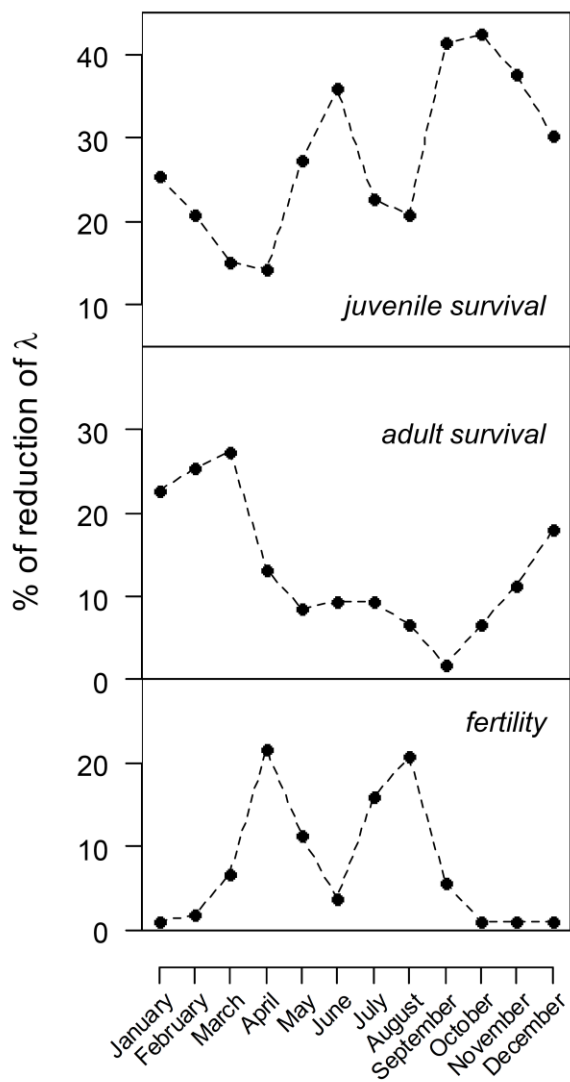
668

669 **Figure 1.** Stable size distributions computed from the population model (in black) and size-distributions observed during the **field-based**
670 **demographic sampling** of the *Gammarus fossarum* population (in grey). J1 and J2 correspond to the two classes of juveniles of the model; A1,
671 A2 and A3 correspond to the three classes of adults.



672

673 **Figure 2.** Reduction in the annual asymptotic population growth rate λ induced by a 10%
674 reduction in juvenile survival rates (s1 and s2), adult survival rates (s3, s4 and s5), fertility (b),
675 growth (r) or a 10% increase in reproductive cycle duration (d) applied simultaneously to each
676 month of the year.



677

678 **Figure 3.** Reduction in annual asymptotic population growth rate λ induced by a 50% reduction
679 in juvenile survival rates (s_1 and s_2), adult survival rates (s_3 , s_4 and s_5) and fertility applied
680 during the different months in the year.

681